The Journal of Engine Research

Journal Homepage: www.engineresearch.ir

Experimental investigations on a pre-chamber spark plug with variable heat range by integrating a controlled hot surface

S. Holzberger[1*], M. Kettner[2], R. Kirchberger[3]

[1] PhD Candidate, Karlsruhe University of Applied Sciences, sascha.holzberger@h-ka.de
[2] Karlsruhe University of Applied Sciences, maurice.kettner@h-ka.de
[3] Graz University of Technology, kirchberger@ivt.tugraz.at

*Corresponding Author

ARTICLE INFO

Article history:
Received: 04 February 2022
Accepted: 19 May 2022

Keywords:
Pre-chamber spark plug
Glow plug
Heat range

ABSTRACT

In gasoline engines, pre-chamber spark ignition systems are used to achieve high efficiency and low NO_x emissions when operating under lean conditions. While a cold pre-chamber spark plug can lead to misfiring and flame quenching under cold start or part load operation, a hot pre-chamber can result in uncontrolled pre-ignition phenomena under full load operation. This paper presents an approach to adjust the heat range of a pre-chamber spark plug and thus, the temperature of the mixture in the pre-chamber, according to the operating condition. Furthermore, higher mixture temperatures in the pre-chamber are intended to enhance the inflammation under lean conditions and to extend the lean limit. For this purpose, a glow plug is integrated into the pre-chamber, whose temperature can be controlled as a function of the operating point. A real-time closed-loop control strategy was applied by using the correlation between the glow plug tip temperature and its electrical resistance. The developed ignition element is called Hot Surface Assisted Spark Ignition (HSASI). In addition to a functional test, a variation of the engine temperature was performed on a single-cylinder, gasoline fueled research engine at the Karlsruhe University of Applied Sciences. In the first step, the influence of the glow plug assistance on the flame development angle and the combustion stability was determined. Subsequently, the air-fuel equivalence ratio λ was varied and the lean limit of unassisted and glow plug assisted spark ignition were determined. Experimental investigations for a constant air-fuel equivalence ratio and a constant ignition timing show that a higher glow plug resistance and thus a higher glow plug temperature shortens the flame development angle and shifts the center of combustion to earlier crank angles. Furthermore, the positive influence of the active glow plug on the flame development angle and the combustion stability increases with retarded ignition timing. With $\lambda = 1.5$ and a constant center of combustion (8 °CA after top dead center firing), the ignition timing can be retarded by 4.5 °CA. When operating with lower coolant temperature, an active glow plug increases combustion stability and extends the lean limit by $\Delta\lambda = 0.1$.

1) Introduction

Combustion process with highly diluted mixtures can contribute to the pursuit of efficient and low-emission internal combustion engines. Mixture dilution reduces combustion temperature, which results in lower NO_x formation and wall heat losses. The dilution can be implemented by leaning as well as by exhaust gas recirculation (EGR). Both methods enable de-throttling and a reduction of pumping losses. Comparing the two possibilities, EGR dilution seems to be the favourable method regarding the simple exhaust gas aftertreatment by a three-way catalyst under stoichiometric conditions. In contrast, dilution by leaning results in higher thermal efficiency. The biggest drawbacks of mixture dilution are the increased ignition energy demand and the lower laminar flame velocity [1, 2]. Slow flame front velocities cause longer combustion duration and increase the probability of engine knocking as well as the cycle-by-cycle variations [3]. A possibility to compensate for these disadvantages in spark ignition engines is the use of pre-chamber spark plugs [4]. A small quantity of mixture is ignited in a pre-chamber, which is connected to the main combustion chamber via orifices. Depending on the design, flame torches or gas jets consisting of hot radical species exit those orifices and penetrate the combustion chamber [5, 6]. This process provides high ignition energy to the diluted mixture in the main combustion chamber and creates turbulence that increases flame speed. Pre-chamber spark plugs can be divided into passive and active ones [4, 7]. An active pre-chamber uses auxiliary pre-chamber fueling to enhance inflammation in the pre-chamber and intensify the gas jets penetrating into the main combustion chamber. Thus, the lean limit and combustion stability can be enhanced compared to passive pre-chamber spark plugs [8]. A major disadvantage of active pre-chamber spark plugs is the higher complexity. An additional fuel supply is needed and more space is demanded. While having less space requirements, passive pre-chamber spark plugs have to ignite the mixture with higher dilution within the pre-chamber resulting in poorer inflammation. A drawback of pre-chamber spark plugs is their large surface-to-volume ratio which favours heat transfer. Under low load and cold start, flame quenching may occur, whereas pre-ignition due to a hot pre-chamber takes place under high loads [8, 9]. Also, hot residual gas, which is trapped in the pre-chamber, can result in undesired pre-ignition. Sotiropoulou et al. [10, 11] suggest additional orifices for scavenging the pre-chamber and avoid possible hot spots within the pre-chamber. Different materials or active cooling represent further possibilities to influence the thermal behaviour of the pre-chamber [12, 13]. In addition, an auxiliary heating device can rise the temperature of the pre-chamber under cold start, low load and idle [8, 14]. Mixture temperature within the pre-chamber has also a great influence on the inflammation process and the combustion stability [13].

In this work an approach for a pre-chamber spark plug with an additional glow plug, which protrudes into the pre-chamber, is presented. The glow plug is controlled by a real-time system and its resistance is used as the controlling parameter. The integration of this auxiliary heating device aims for:

- an enhanced combustion stability under lean operating conditions,
- a faster inflammation process within the pre-chamber,
- an extension of the lean limit,
- higher combustion stability under cold engines,

and is called Hot Surface Assisted Spark Ignition (HSASI).

1-1) Spark plug prototype

In the following, the general design of the developed pre-chamber spark plug is described. The section is divided into a physical and an electrical part. For a more detailed description of the design, refer to [15].

1-2) Spark plug body

The main part of the pre-chamber spark plug is the housing made of steel type S355. It surrounds the ceramic body of a conventional spark plug type ER9EH from NGK and in addition, the ceramic glow plug type CGP003 from BERU. Both ignition elements protrude into a pre-chamber, which is closed off by a nickel cap (see Figure 1). The pre-chamber has a volume of 933 mm^3 and five orifices which are divided into four radial and one central orifice. The orifices have a diameter of 1.2 mm. This yields to a pre-chamber volume (V_{PC}) to compression volume ratio of 4.3% and a total orifice area to V_{PC} of 0.06 cm^{-1}.

To move the location of the spark further into the center of the pre-chamber, the center electrode is extended with a platinum wire. It has a diameter of 1 mm and is also used as mass electrode which is located at the side wall of the pre-chamber. The electrode gap is set to 0.7 mm.

Figure 1: HSASI ignition element (left side) and insight into the pre-chamber with spark plug and glow plug (right side)

1-3) Electric components

The electric connection to the prototype is divided into a high voltage connection for the spark plug and a low voltage part for controlling the ceramic glow plug (CGP). An ignition coil type ZSE 032 from BERU provides the ignition voltage. Due to the limited space, a cable extension was installed instead of using a plug connector. The CGP is connected to a power supply from Delta Elektronika (model SM 18-50) with a maximum voltage of 18 V and maximum current of 50 A. To keep the CGP tip temperature ($T_{CGP,tip}$) constant for an operating point, the electrical resistance of the glow plug R_{CGP} is used as the controlling parameter. This control strategy is based on the assumption that R_{CGP} correlates with $T_{CGP,tip}$. In [15], a resistance- temperature (R-T) correlation was measured in a separate component test rig. $T_{CGP,tip}$ was measured for the HSASI ignition element without pre-chamber cap to enable temperature measurement with the help of a pyrometer. Results are presented in Figure 2. The correlation can be assumed to be linear but is highly sensitive to the mounting condition and the temperature of the surrounding parts which makes a prediction of the real $T_{CGP,tip}$ under engine operation difficult. For this reason, the following investigations focus on R_{CGP}. The PI-controller of Scholl [16] is implemented in the real-time system ADwin Gold II, which sets the CGP voltage (U_{set}) and communicates with the power supply via an analogue high-speed programming and monitoring interface. The actual values of the CGP voltage (U_{CGP}, corresponds to U_{set}) and the current I_{CGP} are monitored by the power supply, R_{CGP} is calculated by ADwin Gold II. The controller frequency is set to 200 Hz with 10 V as a maximum value for U_{set}. At an engine speed of 2500 1/min the controller frequency is equivalent to approximately 10 controller interventions per cycle. Since the maximum operating voltage of the CGP in continuous operation is 7 V and damage to the glow plug should be avoided, the upper limit of R_{GCP} for each operating point is set to a value at which the maximum average voltage U_{set} does not exceed a value of 6 V (1 V up to the maximum voltage as safety buffer).

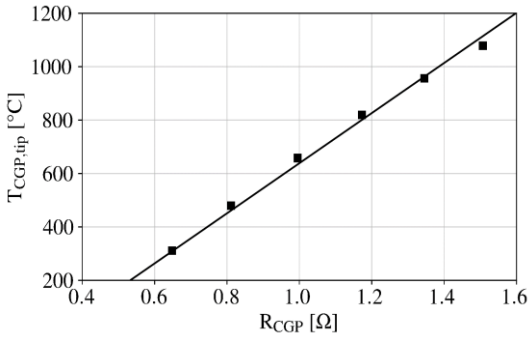

Figure 2: R-T correlation for the HSASI ignition element (without pre-chamber cap) which is mounted into a separate test rig outside of the engine [15]

2) Experimental setup

This section provides an overview of the engine used for the experimental investigations and the measurement setup, which is employed on the test bed.

2-1) Engine specification

The experiments were conducted on a naturally aspirated single-cylinder engine based on the Hatz 1B20 which was chosen on the basis of availability and cost. In order to study the spark ignited combustion the original diesel engine was converted into a gasoline engine through several design changes. The injector bore was machined so that it can be used as a spark plug shaft with a standard M14x1.25 thread. A gasoline low-pressure port fuel injector and a throttle were integrated into the manifold. Fuel pressure is set to 3 bar and end of injection to 300 °CAbTDCf. To decrease the compression ratio the omega shaped piston bowl was transformed into a coin shaped one. In addition, the piston crown was reduced by 1.8 mm which increased the clearance height and resulted in a compression ratio of 11.4. For more precise temperature control, the cylinder head was modified from air

cooled to water cooled by adding a coolant channel to the cylinder head. A radiator with a controlled fan was used to control the coolant temperature. It should be noted that the cylinder is still air-cooled and thus, its temperature varies for different operation points. The engine is controlled by the real time system ADwin Pro. Processes that control fuel injection and ignition timing (IT) run with 125 kHz. The crank angle decoder, which is also used for the in-cylinder pressure indication system, has a resolution of 0.1 °CA. An electric machine is connected to the engine, which serves as starter and generator and allows for variable engine speeds. The engine specification are shown in Table 1.

Table 1: Single-cylinder test bed engine

Engine type (basis)	Hatz 1B20
Max. speed	3600 1/min
Geo. compression ratio	11.4
Stroke/ Bore	62/ 69 cm^3
Displacement volume	232 cm^3
Number of values	2
Injection	Port fuel injection
Fuel	RON95 E5

2-2) Measurement setup

Low frequency data, e.g. coolant temperature, is sampled by the real time system ADwin Pro with a time interval of 1.5 s. All temperatures were measured by type K thermocouples. A Siemens Sitrans P200 pressure sensor measures the manifold pressure (p_{man}). The air-fuel equivalence ratio (λ) is measured by a wide band lambda sensor LSU 4.9. For determining crank angle-based data a DEWETRON DEWE-800-CA indication system is used. In-cylinder pressure is measured by a Kistler sensor (6125C11). Indication systems includes the sampling of the glow plug voltage and glow plug current. For steady-state measurements at different operating points, accuracies of the mean value and maximum standard deviations σ_{max} of the measurands apply as shown in Table 2.

Table 2: Accuracy and standard deviation of measurand

Measurand	Unit	Accuracy	σ_{max}
$T_{C,out}$	K	±0.25	±0.05
λ	-	±0.01	±0.005
CA50	°CAaTDCf	±0.5	±2.0
IMEP	bar	±0.04	±0.16
p_{man}	mbar	±2.0	±0.65

3) Results

Unless otherwise stated, each operating point was measured three times. For every measuring point 200 consecutive cycles were sampled, resulting in 600 cycles per operating point. The net heat release was calculated according to Heywood [17]. Load and manifold pressure were set up by adjusting the throttle. Intake air mass flow was not conditioned resulting in slightly different intake temperatures for each operating point. Coolant outlet temperature is set to 70 °C. After functional testing of the HSASI ignition element, the influence of R_{CGP} on different parameters, e.g. flame development angle ($\Delta\Theta_d$, crank angle interval between ignition timing and crank angle where 5 % of the total net heat was released), lean limit and ignition timing were tested. In addition a variation of the coolant temperature was conducted. The main focus of the experimental investigations presented is on charge dilution. Since no EGR system has yet been implemented in the test bed, only operating points with $\lambda > 1$ were measured.

3.1) Influence of the CGP on combustion

To validate the influence of the glow plug on the inflammation process in the pre-chamber, 600 consecutive cycles were sampled. The engine is running with spark ignition only and constant ignition timing of 11.25 °CAbTDCf (crank angle before top dead center firing) before glow plug controlling was enabled after 200 cycles. It is expected that an active glow plug heats up the pre-chamber and the mixture within the pre-chamber, causing a faster inflammation and combustion. Figure 3 shows the center of combustion CA50 (net heat release), the actual and the set value of R_{CGP} over time. CA50 represents the crank angle where 50 % of the total net heat was released and is depicted as moving average for a period of 25 cycles. R_{CGP} is the average value for each cycle. After 200 cycles a glow plug resistance of 1.573 Ω was set, which corresponds to an average U_{CGP} of approximately 6 V. The rather slow rise in R_{CGP} after enabling glow plug controlling is due to the thermal inertia of the CGP itself as well as to the limitation of the maximum voltage U_{set} (i.e. U_{CGP}) to protect the CGP from overheating. CA50 starts to move towards earlier crank angle before the set value $R_{CGP,set}$ is reached. The reason for this is the faster heat up of the CGP tip right after activation of the

resistance control. The hot CGP shifts combustion to earlier crank angles and causes earlier CA50. Because R_{CGP} is the overall resistance of the GCP, its tip temperature decreases after few seconds when the glow plug body and the metallic leads between push on connector and ceramic tip heat up too. Thus, resistances of the metallic leads increases causing resistance of the ceramic tip decrease in order to keep R_{CGP} constant (see also [15]). As a result, the CGP tip cools down and CA50 moves to later crank angles again. However, CA50 remains at approximately 1 °CA earlier crank angle timings compared to the operation with non-active CGP.

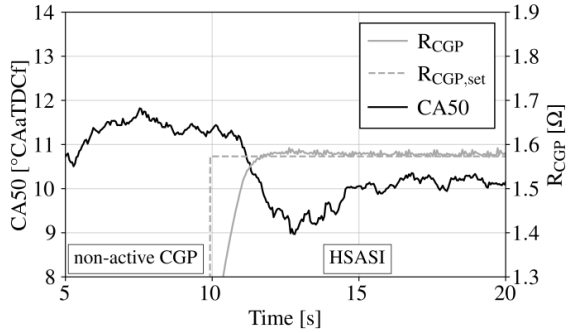

Figure 3: Course of CA50 and R_{CGP} over time with glow plug activation during operation for 2500 rpm, λ = 1.43, IT = 11.25 °CAbTDCf, IMEP = 6 bar and R_{CGP} = 1.573 Ω.

Experiments were repeated for different R_{CGP} to determine the sensitivity of CA50 to R_{CGP}. Results are presented in Figure 4.

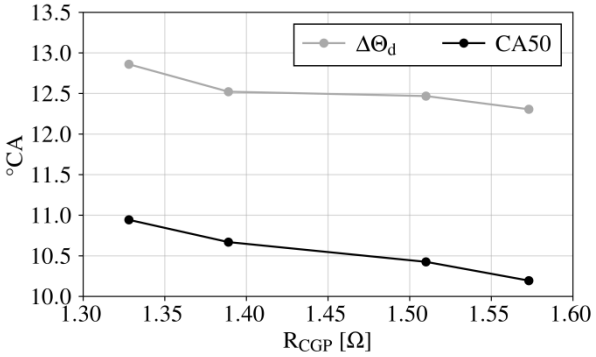

Figure 4: $\Delta\Theta_d$ and CA50 for different R_{CGP} and 2500 rpm, λ = 1.43, IT = 11.25 °CAbTDCf, IMEP = 6 bar.

CA50 and $\Delta\Theta_d$ are plotted over different R_{CGP}. Air-fuel equivalence ratio and ignition timing were kept constant. It can be seen that CA50 moves to earlier crank angles with higher R_{CGP}. This indicates a faster combustion with higher R_{CGP} which also becomes apparent when regarding the flame development angle. A higher R_{CGP} results in a shorter flame development angle and therefore in earlier CA50. Figure 5 shows the traces of the controller parameter for one cycle. Every controller intervention is marked by an adjustment of U_{set}. The maximum voltage step is 0.5 V. The current I_{CGP} follows U_{set} with an overshoot, causing peaks in the trace of R_{CGP}. At -45 °CAaTDCf (crank angle after top dead center firing) glow plug resistance begins to drop until ignition timing is reached. Afterwards it raises again and stays above $R_{CGP,set}$. On the one hand, cold fresh mixture penetrates the pre-chamber with high velocity under a relatively high pressure which leads to an enhanced heat transfer to the gas and cools down the CGP tip. In addition, the heat which is released during combustion heats up the CGP tip causing higher R_{CGP} for crank angle CA > 25 °CAaTDCf. On the other hand, charging and discharging of the ignition coil as well as the break down phase influence the monitoring of I_{CGP} and U_{CGP}. This impedes the analysis of R_{CGP} trace with regard to the flow and heat release inside the pre-chamber.

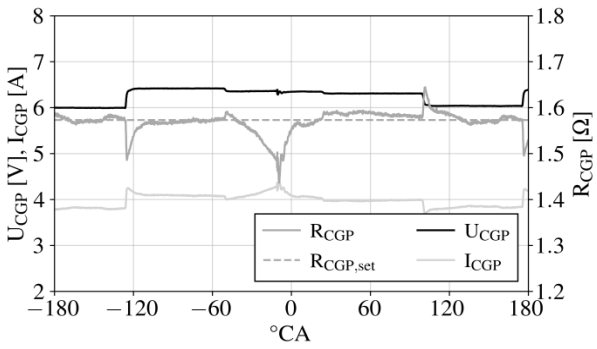

Figure 5: Traces of U_{CGP}, I_{CGP} and R_{CGP} for 2500 rpm λ = 1.43, IT = 11.25 °CAbTDCf, IMEP = 6 bar and R_{CGP} = 1.573 Ω.

Besides the level of R_{CGP}, the time that the glow plug has to heat up the pre-chamber and the mixture within the pre-chamber is also expected to have an influence on the inflammation process. Therefore, a variation of ignition timing was carried out with constant indicated mean effective pressure (IMEP) and R_{CGP}. Figure 6 shows the flame development angle for different ignition timings. It can be seen that the flame development angle increases for later ignition timings with a non-active CGP. An active CGP shortens the crank angle interval of the flame development angle for all ignition timings compared to the non-active one. Also, the flame

development angle seems to increase only slightly for retarded ignition timings under HSASI operation. This leads to the conclusion that the influence of the CGP increases with later ignition timing. The flame development angle is shortened with an activated CGP by 0.5 °CA for an ignition timing of 18.75 °CA, while it is 1.5 °CA for a retarded ignition timing of 9 °CA.

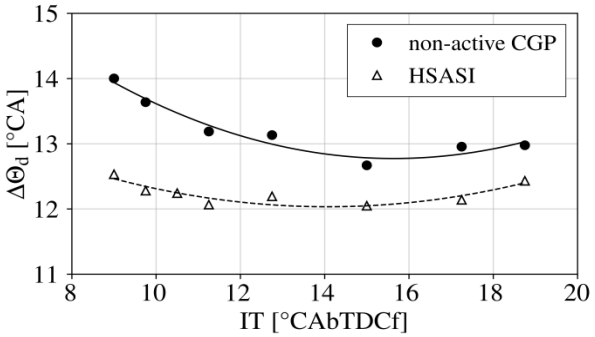

Figure 6: Influence of HSASI on the flame development angle for different ignition timings at 2500 rpm, λ = 1.43 and R_{CGP} = 1.573 Ω.

Figure 7 depicts the standard deviation of the start of combustion (SOC, crank angle where 5 % of the total net heat was released) which indicates the stability of the inflammation. The parameter σ_{SOC} and therefore the cycle-to-cycle variations are highest for late ignition timing when CGP is not activated. In contrast, σ_{SOC} decreases under HSASI operation with retarded ignition and remains on a constant level even when σ_{SOC} increase for operating points with non-active CGP. This emphasizes the positive influence of the hot CGP on the inflammation stability.

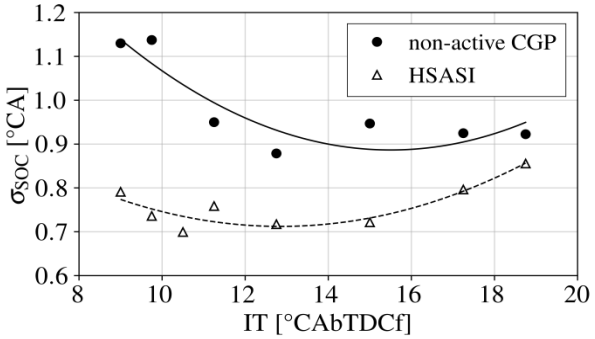

Figure 7: Influence of HSASI on σ_{SOC} for different ignition timings at 2500 rpm, λ = 1.43 and R_{CGP} = 1.573 Ω.

3-2) Variation of air-fuel equivalence ratio

Figure 8 shows the ignition timing for different λ for constant IMEP and CA50. Experiments were conducted for lean operating points only. Starting with a λ of 1.3, mixture was leaned until the lean limit was reached. The lean limit is defined as the point where the coefficient of variation COV_{IMEP} exceeded a value of 5 %. COV_{IMEP} is the ratio of the standard deviation of IMEP to its mean value. For higher λ, ignition timing has to be advanced to reach constant CA50 of 8 °CAaTDCf. Comparing the different operating modes, it can be seen that the active CGP enables later ignition timings. While the difference in ignition timing is rather small for a λ of 1.3 with 0.75 °CA, it becomes greater for leaner mixtures. At λ = 1.5, ignition timing can be retarded by 4.5 °CA with an active CGP. Furthermore, the lean limit is extended by 0.05 for HSASI operation. As expected, the greatest potential for the use of HSASI is in lean operation.

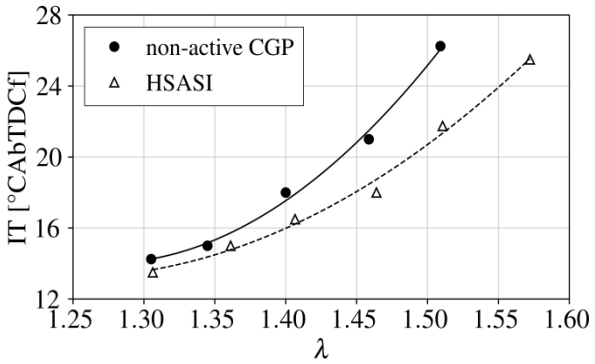

Figure 8: Influence of HSASI on ignition timing for different λ at 2500 rpm, CA50 = 8 °CAaTDCf, IMEP = 6 bar and R_{CGP} = 1.573 Ω.

3-3) Variation of coolant temperature

To determine further potential of the HSASI ignition element under part load and lower engine temperatures, coolant outlet temperature ($T_{C,out}$) was decreased from 70 °C to 45 °C. This drops the average cylinder temperature by about 20 °C. Figure 9 shows COV_{IMEP} over lean mixtures. Experiments were conducted for both operating modes until lean limits were reached. COV_{IMEP} increases with higher λ values. For low values of λ, $T_{C,out}$ seem to have no influence on combustion stability. An active CGP decrease COV_{IMEP} for leaner mixtures and enabling further leaning of the mixture even with lower $T_{C,out}$. The lean limit is extended for the HSASI operation by approximately 0.1 comparing to a non-active CGP for lower coolant temperatures.

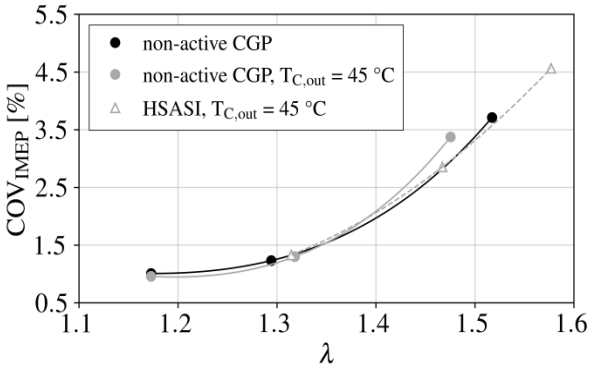

Figure 9: Influence of HSASI on COV_{IMEP} and lean limit for lower coolant temperature at 1800rpm, CA50 = 8°CAaTDCf and p_{man} = 887 mbar.

4) Conclusion

In this work experimental investigations on a pre-chamber spark plug with an integrated ceramic glow plug are presented. The developed ignition element is called Hot Surface Assisted Spark Ignition (HSASI). The CGP is controlled by a real-time closed-loop control strategy. Based on the assumption of a R-T-correlation, the glow plug resistance is used as a controlling parameter to adjust the glow plug tip temperature. The upper limit of R_{CGP} is defined by the maximum average voltage applied to the CGP. This voltage limit is implemented due to the operating limit of the CGP and protects the CGP from damage. The effects of the active CGP on the combustion are the following:

- For a constant air-fuel equivalence ratio and ignition timing, higher R_{CGP} shortens the flame development angle and shifts CA50 to earlier crank angles.
- The positive influence of the active CGP on the flame development angle and the combustion stability increases with retarded ignition timings.
- The influence of the active CGP increases for higher values of λ. Ignition timing can be retarded by 0.75 °CA for λ = 1.3 and 4.5 °CA for λ = 1.5.
- HSASI operation shows higher combustion stability under lower coolant temperature and lean limit is extended by 0.1.

For future work, the test bed engine will be extended with an EGR system to validate the potential of the HSASI ignition element under different EGR rates.

Acknowledgment

The present work was part of the project "ReKra". The authors would like to thank the Baden-Wuerttemberg Ministry of Economy, Labour and Housing for the financial support of the project. Further, the authors thank Mr. Gion Heugel and Mr. Daniel Exter of the Gas Engine Laboratory at the UAS Karlsruhe for the support in the development of the ignition element and in conducting the measurements.

Nomenclature

CA	Crank angle
CAaT DCf	Crank angle after top dead center firing
CAbT DCf	Crank angle before top dead center firing
CA50	Crank angle at which 50 % of the heat was released (net release)
CGP	Ceramic glow plug
COV	Coefficient of variation
HSASI	Hot Surface Assisted Spark Ignition
IT	Ignition timing
I_{CGP}	Glow plug current, A
IMEP	Indicated mean effective pressure, bar
p_{man}	Manifold pressure, mbar
R-T	Resistance-temperature
R_{CGP}	Glow plug resistance, Ω
$R_{CGP,set}$	Set value of R_{CGP}, Ω
SOC	Start of combustion
$T_{CGP,tip}$	Glow plug tip temperature, °C
$T_{C,out}$	Coolant outlet temperature, °C
U_{CGP}	Glow plug voltage, V
U_{set}	Glow plug voltage set by controller, V
V_{PC}	Pre-chamber volume, mm^3
$\Delta\Theta_d$	Flame development angle, °CA
λ	Air-fuel equivalence ratio
σ	Standard deviation

References

[1] Kettner, M. "Zündsysteme für magere Gemische", Study for the Forschungsvereinigung Verbrennungskraftmaschinen(FVV)e.V., 2004.

[2] Amirante, R., Distaso, E., Tamburrano, P. and Reitz, R.D., "Laminar flame speed correlations for methane, ethane, propane and their mixtures, and natural gas and gasoline for spark-ignition engine simulations" International Journal of Engine Research 18(9): p. 951-970, 2017, doi:10.1177/1468087417720018.

[3] Ozdor, N., Dulger, M., and Sher, E., "Cyclic Variability in Spark Ignition Engines - A

Literature Survey," 940987, SAE Technical Paper, 1994, doi:10.4271/940987.
[4] Müller C., Morcinkowski B., Schermus C., Habermann K. et al., "Development of a Pre-chamber for Spark Ignition Engines in Vehicle Applications," in: Ignition Systems for Gasoline Engines: 4th International Conference, December 6-7: p. 261-274.
[5] Wöbke, M., Reinicke, P.-B., Rieß M., von Römer L. et al., "Characterization of the Ignition and Early Flame Propagation of Pre-Chamber Ignition System in a High-Pressure Combustion Cell" in: Ignition Systems for Gasoline Engines: 4th International Conference: p. 385-423.
[6] Wang, B. and Wang, Z., "Experimental Research on Pre-chamber Jet Ignition in Rapid Compression Machine and Natural Gas Engine," in: Ignition Systems for Gasoline Engines: 4th International Conference: p. 424-441.
[7] Toulson, E., Schock, H.J., and Attard, W.P., "A Review of Pre-Chamber Initiated Jet Ignition Combustion Systems," SAE International, 2010, doi:10.4271/2010-01-2263.
[8] Sens, M. and Binder E., "Vorkammerzündung als Schlüsseltechnologie für einen zukünftigen Antriebsstrang-Mix," MTZ Motortechnische Zeitschrift 80(02): p. 46-53, 2019.
[9] Kettner, M., "Experimentelle und numerische Untersuchungen zur Optimierung der Entflammung von mageren Gemischen bei Ottomotoren mit Direkteinspritzung," Ph.D. Thesis, Universität Karlsruhe, 2006.
[10] Sotiropoulou, E., Knepper S., Deeken, S., and Grewe, F., "Zero Emission-Die Evolution von Erdgas zu Wasserstoff mit Vorkammerzündkerzen," MTZ Motortechnische Zeitschrift: p. 50-55, 2020, doi:10.1007/s35146-020-0231-y.
[11] Sotiropoulou, E. and Tozzi, L., "Active Scavenge Prechamber," PCT/US2014/024904, 2016.
[12] Sens, M., Binder E., Benz A., Krämer L. et al., "Pre-Chamber Ignition as a Key Technology for Highly Efficient SI Engines – New Approaches and Operating Strategies," in: 39. Wiener Motorensymposium.
[13] Takashima, Y., Tanaka, H., Sako, T., and Furutani, M., "Evaluation of Engine Performance and Combustion in Natural Gas Engine with Pre-Chamber Plug under Lean Burn Conditions," SAE Int. J. Engines 8(1): 221–229, 2015, doi:10.4271/2014-32-0103.
[14] Marko F. and Koenig G., "Zuführungs- und Zündvorrichtung für einen Gasmotor und Verfahren zum Betrieb einer Zuführungs- und Zündvorrichtung für einen Gasmotor," DE 10 2017 009 607 A1.
[15] Holzberger S., Kettner M., and Kirchberger R., "Hot Surface Assisted Spark Ignition (HSASI) - An Approach to Vary the Heat Range of Spark Plugs during Operation" Reports on Energy Efficient Mobility, 2021.
[16] Scholl, F., "Study of Premixed Combustion Induced by Controlled Hot Surface Ignition in Stationary Gas Engines," Ph.D. Thesis, University of Valladolid & Hochschule Karlsruhe, 2017.
[17] Heywood, J., "Internal Combustion Engine Fundamentals," McGraw-Hill, ISBN 0-07-028637-X, 1988.

فصلنامهٔ علمی تحقیقات موتور

تارنمای فصلنامه: www.engineresearch.ir

بررسی تجربی شمع پیش-محفظه با محدوده حرارتی متغیر با ترکیب سطح داغ کنترل شده

ساسچا هولزبرگر[۱*]، موریس کتنر[۲]، رولند کرچبرگر[۳]

[۱] دانشجوی دکتری، دانشگاه علوم کاربردی کارلسروهه، sascha.holzberger@h-ka.de

[۲] دانشگاه علوم کاربردی کارلسروهه، maurice.kettner@h-ka.de

[۳] دانشگاه صنعتی گراتس، kirchberger@ivt.tugraz.at

[*] نویسندهٔ مسئول

چکیده

در موتورهای بنزینی، سیستم‌های اشتعال جرقه‌ای پیش-محفظه برای دستیابی به راندمان بالا و انتشار کمتر NOx هنگام کار در شرایط مخلوط فقیر استفاده می‌شوند. در حالی که شمع پیش-محفظه سرد می‌تواند منجر به احتراق ناقص و خاموش شدن شعله در هنگام شروع سرد یا شرایط بخش بار شود، یک پیش-محفظه داغ می‌تواند منجر به پدیده‌های کنترل نشده پیش-اشتعال تحت بار کامل شود. این مقاله رویکردی را برای تنظیم محدوده حرارتی شمع پیش-محفظه فلذا دمای مخلوط در پیش-محفظه، با توجه به شرایط کاری ارائه می‌کند. علاوه بر این، دماهای بالاتر مخلوط در پیش-محفظه برای تسهیل احتراق در شرایط مخلوط فقیر و گسترش حد فقیری در نظر گرفته می‌شود. برای این منظور، یک شمع نقطهٔ ملتهب (glow) درون پیش-محفظه قرار می‌گیرد که دمای آن را می‌توان به عنوان تابعی از نقطه کاری کنترل کرد. یک استراتژی کنترل حلقه بسته بلادرنگ با استفاده از همبستگی بین دمای نوک شمع نقطهٔ ملتهب و مقاومت الکتریکی آن اعمال شد. المان احتراق توسعه یافته، اشتعال جرقه‌ای با کمک سطح داغ (HSASI) نامیده می‌شود. علاوه بر آزمایش عملکردی، تغییر دمای موتور روی یک موتور تحقیقاتی تک سیلندر با سوخت بنزینی در دانشگاه علوم کاربردی کارلسروهه انجام شد. در مرحله اول، تأثیر کمک شمع نقطهٔ ملتهب بر زاویه گسترش شعله و پایداری احتراق تعیین شد. پس از آن، نسبت هم‌ارزی هوا-سوخت λ تغییر کرد و حد فقیری اشتعال جرقه‌ای بدون/با کمک شمع نقطهٔ ملتهب تعیین شد. بررسی‌های تجربی برای نسبت هم‌ارزی ثابت هوا به سوخت و زمان‌بندی ثابت اشتعال نشان می‌دهد که مقاومت بالاتر شمع نقطهٔ ملتهب در نتیجه دمای بالاتر شمع نقطهٔ ملتهب، زاویه گسترش شعله را کوتاه و مرکز احتراق را به زوایای جلوتر میل‌لنگ انتقال می‌دهد. علاوه بر این، تأثیر مثبت شمع نقطهٔ ملتهب فعال بر روی زاویه گسترش شعله و پایداری احتراق با تأخیر زمان‌بندی احتراق افزایش می‌یابد. با $\lambda = 1.5$ و مرکز ثابت احتراق (۸ درجه میل‌لنگ پس از نقطه مکث بالا)، زمان اشتعال می‌تواند تا ۴٫۵ درجه میل‌لنگ به تأخیر افتد. در هنگام کار با دمای پایین‌تر سیال خنک‌کننده، یک شمع نقطهٔ ملتهب فعال پایداری احتراق را افزایش می‌دهد و حد فقیری سوخت را به میزان $\Delta\lambda = 0.1$ افزایش می‌دهد.

اطلاعات مقاله

تاریخچهٔ مقاله:

دریافت: ۱۵ بهمن ۱۴۰۰

پذیرش: ۲۹ اردیبهشت ۱۴۰۱

کلیدواژه‌ها:

شمع پیش-محفظه

شمع سوزان

محدودهٔ حرارتی